The cytological and electrophysiological effects of silver nanoparticles on neuron-like PC12 cells

Ze-Qun Zhang
Southeast University
Chen Meng
Southeast University
Kun Hou
Southeast University
Zhi-Gong Wang
Southeast University
Yan Huang
Southeast University
Xiao-Ying Lü (luxy@seu.edu.cn)
Southeast University

Research Article

Keywords: Silver nanoparticle, Cytotoxicity, Electrical excitability, Voltage threshold measurement method, High content analysis techniques

Posted Date: April 11th, 2022

DOI: https://doi.org/10.21203/rs.3.rs-1453101/v1

Abstract

Background

Silver nanoparticles (SNPs) are widely used in a large number of products. SNPs can cross the blood-brain barrier and are subsequently deposited continuously in the brain, causing a variety of pathological responses and diseases. As a result, the toxic effects of SNPs on the nervous system have attracted considerable attention, but the mechanism of toxicity remains unclear. Moreover, neurons have different cytological and electrophysiological properties, and their functions are highly dependent on changes in electrophysiological properties.

Results

Different concentrations of SNPs (20 nm) were prepared, and the effects of different application durations on the cell viability and electrical excitability of rat adrenal pheochromocytoma (PC12) quasi-neuronal networks were investigated. The effects of 200 μM SNPs on the neurite length, cell membrane potential (CMP) difference, intracellular Ca^{2+} content, mitochondrial membrane potential (MMP) difference, adenosine triphosphate (ATP) content, and reactive oxygen species (ROS) content of networks were investigated. The results showed that 200 μM SNPs produced grade 1 cytotoxicity at 48 h of interaction, and the other concentrations of SNPs were noncytotoxic. Noncytotoxic 5 μM SNPs significantly increased the electrical excitability of PC12 quasi-neuronal networks, and noncytotoxic 100 μM SNPs led to an initial increase followed by a significant decrease in electrical excitability. While cytotoxic 200 μM SNPs significantly decreased the electrical excitability. 200 μM SNPs led to decreases in neurite length, MMP difference and ATP content and increases in CMP difference, and intracellular Ca^{2+} and ROS levels with increasing interaction time.

Conclusions

The results above revealed that using only cell viability to evaluate nanoparticles-induced neurotoxicity is partial. Therefore, not only cell viability but also electrophysiological properties should be considered when evaluating nanoparticles-induced neurotoxicity. The SNPs-induced cytotoxicity mainly originated from its effects on ATP content, cytoskeletal structure and ROS content. The SNPs-induced decrease in electrical excitability could be explained by a decrease in ATP content which could lead to cellular energy deficiency that opened K_{ATP} channels on the cell membrane, resulting in an increase in the CMP difference and hyperpolarization. ATP content may thus be an important indicator of both cell viability and electrical excitability of PC12 quasi-neuronal networks.

Background

Due to their excellent antibacterial properties, silver nanoparticles (SNPs) are widely used in a large number of products such as food packaging, air filters, disinfectants, cosmetics, antibacterial gels, trauma dressings and cardiovascular implants [1, 2]. SNPs can enter the circulatory system through oral administration, inhalation, dermal contact and intravenous injection. SNPs smaller than 35 nm in diameter can cross the blood-brain barrier [3] and are subsequently deposited continuously in the brain, causing a variety of pathological responses and diseases [4]. As a result, the toxic effects of SNPs on the nervous system have attracted considerable attention, but the mechanism of toxicity remains unclear.

Unlike normal somatic cells, neurons have different cytological and electrophysiological properties, and their functions are highly dependent on changes in electrophysiological properties [5]. Therefore, we believe that to fully understand the toxicity of SNPs to neurons, both cytological and electrophysiological properties should be comprehensively investigated. However, most of the current studies have focused on the cytological effects of SNPs [6], while very few studies investigated their electrophysiological effects on neurons [7].

It is well known that reception, processing and transmission of information in neuronal networks is the basis of higher brain activities, so studying the electrical excitability of neuronal networks is an effective way for investigating the effects of exogenous factors on brain function in electrophysiological studies. A microelectrode array (MEA) can effectively record the electrical signals of neuronal networks without damaging the neurons [8]. Moreover, measuring electrophysiological characteristics, such as the discharge frequency, of neuronal networks cultured on MEAs has been proven to be an effective method for evaluating the toxic effects of exogenous factors (e.g. nanoparticles, etc.) on neurons [9]. Our group previously proposed an MEA-based voltage threshold measurement method (VTMM) to quantify the effects of exogenous factors on electrical excitability of neuronal networks. VTMM is similar to the rheobase measurement with patch clamp, and both evaluate the electrical excitability by measuring the minimum stimulus that causes excitation [10, 11]. Similar to the rheobase measurement, the lower the voltage threshold (V_{Th}) is in VTMM, the higher the electrical excitability is, and vice versa. However, in contrast to the rheobase method, which measures individual neurons, VTMM measures the electrical excitability of a neuronal network. The validity of the VTMM has been verified in our previous studies of hippocampal neuronal networks and hippocampal brain slices [11, 12].

However, the use of primary cultured neurons has several disadvantages such as complexity of extraction, individual variation and potential failure to comply with the 3R (Reduction, Refinement and Replacement) principles for animal protection. In contrast, differentiated rat adrenal pheochromocytoma (PC12) cells are more easily cultured and subcultured. Moreover, PC12 cells not only resemble neurons in terms of cell structure and electrical excitability [13, 14], but are also capable of forming quasi-neuronal networks [15]. Therefore, these cells have been widely used in nanoparticle-induced cytotoxicity and electrophysiology studies [16, 17]. Cui et al. used MEAs and fluorescence microscopy to simultaneously monitor action potentials and dopamine release from PC12 cells [18]. Our group demonstrated that the quasi-neuronal networks had similar electrical excitability changes as hippocampal neuronal networks and hippocampal brain slices to acetylcholine, ethanol, lidocaine hydrochloride, and changes in

temperature. Therefore, PC12 cells are recommended as an alternative cell model for studying the cytotoxic and electrical excitability effects of exogenous factors on neurons under certain conditions [19].

The aim of this paper was to investigate the toxic effects of SNPs on PC12 cells in terms of changes in both cytological and electrophysiological properties as well as to determine the underlying mechanism of these effects. The effects of SNPs on the viability of PC12 cells and on the electrical excitability of quasi-neuronal networks were first evaluated by the methyl thiazolyl tetrazolium (MTT) method and VTMM respectively. Studies on six aspects of PC12 cells, namely, neurite length, cell membrane potential (CMP) difference, intracellular Ca^{2+} content, mitochondrial membrane potential (MMP) difference, reactive oxygen species (ROS) content and adenosine triphosphate (ATP) content, were performed subsequently using a high content analysis (HCA) system. The correlations among cell viability, electrical excitability and these six indicators after treatment with SNPs were jointly analysed to elucidate the different mechanisms underlying the SNPs-induced changes in cytological and electrophysiological properties.

Results

Preparation and characterization of SNPs

The transmission electron microscopy (TEM) image (Fig. 1A) and absorption spectra (Fig. 1B) of SNPs showed that the SNPs were spherical with an average size of 21.45 ± 2.72 nm and a maximum absorption wavelength of 389 nm (The dataset is shown in Additional file 1) [20]. The original concentration of SNPs was 1.4 g/L.

Evaluation of SNP cytotoxicity in PC12 cells

The cell viability rates of PC12 cells treated with different concentrations (5, 25, 50, 100 and 200 μM) of 20 nm SNPs for 0.5, 1, 12, 24 or 48 h are shown in Table 1 and Fig. 2. The cell viability rates in all 5 μM SNPs-treated groups were higher than 93%. There was no significant difference between the cell viability rates in the 25, 50 and 100 μM SNPs-treated groups ($P > 0.05$), and the cell viability rates remained high after 48 h in these groups (88.45 ± 2.41%, 88.10 ± 3.61% and 88.27 ± 0.61%, respectively), indicating grade 0 cytotoxicity. In the 200 μM SNPs-treated groups, the cell viability rates were higher than 85% with grade 0 cytotoxicity when the duration of treatment was less than or equal to 24 h; after 48 h, the cell viability rate decreased to 71.29 ± 2.68%, indicating grade 1 cytotoxicity.

Table 1. Cell viability rates of PC12 cells treated with 20 nm SNPs at concentrations of 5, 25, 50, 100 and 200 μM for 0.5, 1, 12, 24 and 48 h. The results are presented as the mean ± standard deviation (SD) (n= 6).

Time (h) Concentration (μM)	0.5	1	12	24	48
5	95.54±2.78	95.86±4.02	93.35±4.20	94.31±2.23	93.74±1.86
25	92.89±5.37	93.91±1.41	89.96±3.07	88.59±2.40	88.45±2.41
50	95.07±1.66	93.14±3.95	89.61±6.55	88.46±2.05	88.10±3.61
100	92.01±1.00	91.36±4.36	89.10±4.55	88.31±3.27	88.27±0.61
200	91.86±2.09	91.29±3.62	87.12±3.90	85.21±0.60	71.29±2.68

Viability rate [81%, 100%] indicates grade 0 cytotoxicity, viability rate [61%, 80%] indicates grade 1 cytotoxicity, viability rate [41%, 60%] indicates grade 2 cytotoxicity, viability rate [21%, 40%] indicates grade 3 cytotoxicity, and viability rate [0, 20%] indicates grade 4 cytotoxicity.

Standard V_{Th} of PC12 quasi-neuronal networks

An image of PC12 quasi-neuronal networks on an MEA is shown in Fig. 3A, demonstrating that PC12 cells were tightly connected to each other on the MEA. One stimulating electrode and three detecting electrodes were randomly selected among the electrodes well covered by cells for experiments. Figure 3B shows the electrical signals of the stimulating and detecting electrodes displayed on the oscilloscope. As shown in Fig. 3B, 57.8 ms after stimulation (negative pulse amplitude of 37 mV) was applied to one normally cultured PC12 quasi-neuronal network, action potentials were recorded at each of the three detecting electrodes. Therefore, the standard V_{Th} of this specific PC12 quasi-neuronal network (shown in Fig. 3) was 37 mV.

According to our previous results, the minimum amplitude of the stimulation pulses that triggered responses from the networks in normal culture environment was defined as the standard V_{Th}. The V_{Th} of networks of the same kind of cells is a fixed value as the test environment remains unchanged [11, 12]. The standard V_{Th} of PC12 quasi-neuronal networks measured in this paper was 36.50 ± 0.58 mV, which was not significantly different ($P > 0.05$) from our previous result (36 ± 2.37 mV) [19].

V_{Th} of PC12 quasi-neuronal networks exposed to SNPs

The V_{Th} of PC12 quasi-neuronal networks treated with 20 nm SNPs at concentrations of 5, 100 or 200 μM for 0.5, 1, 12, 24 or 48 h are shown in Table 2 and Fig. 4.

Table 2
V_{Th} of PC12 quasi-neuronal networks treated with 20 nm SNPs at concentrations of 5, 100 and 200 μM for 0.5, 1, 12, 24 and 48 h. The results are presented as the mean ± SD (n = 4).

Time (h)	0	0.5	1	12	24	48
Concentration(μM)	(Standard V_{Th})					
5	36.50 ± 0.58	32.00 ± 1.83	30.50 ± 1.29	29.00 ± 1.83	31.00 ± 2.16	27.25 ± 1.89
100		33.50 ± 0.58	36.25 ± 0.50	49.25 ± 0.50	75.75 ± 1.26	75.75 ± 0.96
200		37.80 ± 2.68	43.67 ± 1.51	52.00 ± 2.10	85.00 ± 0.71	94.80 ± 3.49

After treatment with 5 μM SNPs, the V_{Th} of PC12 quasi-neuronal networks was significantly lower than the standard V_{Th} at all five time points ($P < 0.05$), with a minimum value of 27.25 ± 1.89 mV at 48 h, which suggests that 5 μM SNPs led to a significant increase in the electrical excitability of PC12 quasi-neuronal networks.

After treatment with 100 μM SNPs, the V_{Th} of the networks was lower than the standard V_{Th} at 0.5 and 1 h and very significantly higher than the standard V_{Th} at 12 h and beyond ($P < 0.01$). This result suggests that 100 μM SNPs led to an increase followed by a significant decrease in the electrical excitability of PC12 quasi-neuronal networks.

After treatment with 200 μM SNPs, the V_{Th} of the networks was higher than the standard V_{Th} at each time point and was very significantly higher than the standard V_{Th} at 1 h and beyond ($P < 0.01$). This result suggests that 200 μM SNPs caused a significant decrease in the electrical excitability of PC12 quasi-neuronal networks after 1 h of treatment.

Neurite length of cells exposed to SNPs

The lengths of neurites of PC12 cells treated with 20 nm 200 μM SNPs for 0.5, 1, 12, 24 or 48 h are shown in Table 3 and Fig. 5. After treatment with 200 μM SNPs, the neurite length decreased gradually and was significantly ($P < 0.05$) lower than that of the control group after 12 h.

Table 3
Neurite length of PC12 cells treated with 20 nm 200 μM SNPs for 0.5, 1, 12, 24 and 48 h. The results are presented as the mean ± SD (n = 6).

Time (h)	0.5	1	12	24	48
Relative neurite length (%)	94.26 ± 14.05	84.93 ± 7.22	78.77 ± 5.74	78.90 ± 9.12	70.78 ± 5.90

CMP difference of cells exposed to SNPs

The CMP differences of PC12 cells treated with 20 nm 200 μM SNPs for 0.5, 1, 12, 24 or 48 h are shown in Table 4 and Fig. 6. The CMP differences in each SNPs-treated group were higher than those in the control group. Within 0–24 h, noncytotoxic concentrations of SNPs induced a sustained increase in CMP difference. At 48 h, a significant decrease in CMP difference was observed compared to that at 24 h ($P < 0.05$). However, at 48 h, the CMP difference was still very significantly higher than that of the control group ($P < 0.01$), and the V_{Th} was still very significantly higher than the standard V_{Th} ($P < 0.01$) (Fig. 4), which suggests that electrical excitability of these networks was still lower than normal.

Table 4
CMP difference of PC12 cells treated with 200 μM SNPs for 0.5, 1, 12, 24 and 48 h. The results are presented as the mean ± SD (n = 6).

Time (h)	0.5	1	12	24	48
Relative CMP difference (%)	102.33 ± 10.71	101.82 ± 2.80	107.40 ± 2.53	120.64 ± 2.45	114.11 ± 2.30

Intracellular Ca^{2+} content of cells exposed to SNPs

The intracellular Ca^{2+} content of PC12 cells treated with 20 nm 200 μM SNPs for 0.5, 1, 12, 24 or 48 h is shown in Table 5 and Fig. 7. The intracellular Ca^{2+} contents in all SNPs-treated groups were higher than those in the control group and were very significantly higher at 24 h (243.96%) and 48 h (221.50%) ($P < 0.01$). Moreover, the intracellular Ca^{2+} content at 48 h was significantly lower ($P < 0.05$) than that at 24 h.

Table 5
Intracellular Ca^{2+} content of PC12 cells treated with 20 nm 200 μM SNPs for 0.5, 1, 12, 24 and 48 h. The results are presented as the mean ± SD (n = 6).

Time (h)	0.5	1	12	24	48
Relative intracellular Ca^{2+} content (%)	105.70 ± 11.16	105.19 ± 13.57	116.35 ± 1.19	243.96 ± 10.01	221.50 ± 23.46

MMP difference, ATP content and ROS content of cells exposed to SNPs

The MMP difference, ATP content and ROS content of PC12 cells treated with 200 μM SNPs for 0.5, 1, 12, 24 or 48 h are shown in Table 6 and Fig. 8. The MMP difference and ATP content of cells exposed to SNPs were very significantly higher ($P < 0.01$) than those of the control groups at 0.5 h of treatment. The MMP difference and ATP content continuously decreased starting at 1 h and were very significantly lower than those of the control group at 24 h and 48 h and at 12 h, 24 h and 48 h, respectively ($P < 0.01$). The ROS content of cells exposed to SNPs continuously increased and was very significantly higher than that of the control group at 24 and 48 h ($P < 0.01$).

Table 6
MMP difference, ATP content and ROS content of PC12 cells treated with 20 nm 200 μM SNPs for 0.5, 1, 12, 24 and 48 h. The results are presented as the mean ± SD (n = 6).

Time (h)	0.5	1	12	24	48
Relative MMP difference (%)	110.68 ± 5.00	96.91 ± 3.92	96.53 ± 0.59	91.98 ± 2.93	91.28 ± 3.18
Relative ATP content (%)	113.92 ± 2.80	98.53 ± 1.58	72.33 ± 5.03	62.82 ± 3.41	55.78 ± 3.82
Relative ROS content (%)	108.55 ± 30.08	110.22 ± 37.44	120.92 ± 17.85	226.78 ± 4.81	510.69 ± 76.18

Conjoint analysis between cytological indicators, cell viability and V_{Th}

A correlation analysis of cell viability and V_{Th} of cells exposed to SNPs revealed a high correlation (r= -0.95). Thus, to discuss the molecular mechanisms of cell viability and V_{Th} variation, the results of cell viability and V_{Th} were analysed conjointly with the results of the above six cytological indicators, and Pearson correlation coefficients were calculated for the relationships between cell viability, V_{Th} and each indicator (Table 7).

Table 7
Pearson correlation coefficients (r) between each cytological indicators, cell viability and V_{Th}

	V_{Th}	ATP content	Neurite length	ROS content	Intracellular Ca^{2+} content	MMP difference	CMP difference
Cell viability	**-0.95**	**0.95**	**0.93**	**-0.90**	**-0.83**	0.77	-0.79
V_{Th}		**-0.92**	**-0.85**	**0.87**	**0.96**	-0.79	**0.91**

|r| = 0.8 to 1.0 indicates high correlation, |r| = 0.5 to 0.8 indicates moderate correlation, |r| = 0.3 to 0.5 indicates low correlation and |r| = 0 to 0.3 indicates very weak or no correlation. Both PC12 cell viability and V_{Th} were highly correlated with ATP content, neurite length, ROS content and intracellular Ca^{2+} content (|r|>0.8), and both were moderately correlated with MMP difference (r = 0.77 and − 0.79). Additionally, V_{Th} was highly correlated with CMP difference (r = 0.91), while cell viability was only moderately correlated with CMP difference (r=-0.79).

Discussion

SNPs smaller than 35 nm are able to cross the blood-brain barrier [3]. The size of SNPs commonly used in clinical practice is generally ~ 20 nm, and SNPs of this size have been used in neurotoxicity studies by

several research groups [21, 22]. Therefore, 20 nm SNPs were selected in this paper to investigate their toxic effects.

In the current paper, the MTT results showed that 200 μM SNPs produced grade 1 cytotoxicity at 48 h of interaction, and the other concentrations of SNPs were noncytotoxic. To investigate the effects of noncytotoxic and cytotoxic concentrations of SNPs on PC12 quasi-neuronal networks and to compare our current findings with our previous work [23], three concentrations of SNPs (5, 100 and 200 μM) were selected for VTMM experiments.

Figure 4 suggests that 5 μM SNPs led to a significant increase in the electrical excitability of PC12 quasi-neuronal networks. And 100 μM SNPs led to an increase followed by a significant decrease in the electrical excitability of the networks. It also suggests that 200 μM SNPs caused a significant decrease in the electrical excitability of the networks after 1 h of treatment.

When comparing Fig. 2 and Fig. 4, it was evident that the noncytotoxic 5 μM SNPs led to a significant decrease ($P < 0.05$) in the V_{Th} of PC12 quasi-neuronal networks at 0.5 h, while noncytotoxic 100 μM SNPs led to a significant increase ($P < 0.01$) in the V_{Th} of the networks at 12 h. This result indicates that SNPs were still able to alter the electrical excitability of PC12 quasi-neuronal networks at noncytotoxic concentrations. Grade 1 cytotoxicity appeared after 48 h of treatment with 200 μM SNPs, yet the V_{Th} was very significantly ($P < 0.01$) higher than the standard V_{Th} after only 1 h, which indicated a reduction in the electrical excitability of PC12 quasi-neuronal networks. Taken together, these results show that the SNPs-induced changes in electrophysiological properties of PC12 cells appeared before the changes in cell viability, suggesting that using cell viability alone to evaluate nanoparticles-induced neurotoxicity is partial. Therefore, not only cell viability, but also electrophysiological properties should be considered when evaluating nanoparticles-induced neurotoxicity.

To further investigate the mechanisms of SNPs-induced cytotoxicity and changes in electrical excitability, changes in six aspects of PC12 cells, namely, neurite length, CMP difference, intracellular Ca^{2+} content, MMP difference, ROS content and ATP content were studied under the effect of 200 μM cytotoxic SNPs.

On the one hand, the presence of neurites is a prerequisite for the formation of synapses, which are the basis of signaling between neurons. In addition, a relatively high density of voltage-gated sodium channels, which play an important role in the production and conduction of neural signals, are distributed along the axon initiation segment of neurons [24]. Decreased neurite length might shorten the axon initiation segment, therefore leading to a decrease in the number of sodium channels, which in turn would affect neurotransmitter release and reduce the electrical excitability of neuronal networks [12]. On the other hand, decreased neurite length correspond to cell damage, particularly cytoskeletal damage [25]. Thus, the SNPs-induced decrease in neurite length (Fig. 5) suggests that SNPs caused cytoskeletal damage and this decrease might affect signaling between neuron-like PC12 cells.

The CMP is one of the most important indicators of cell survival, as a decrease in CMP difference is usually accompanied by toxic effects, apoptosis and necrosis [26]. Additionally, the CMP difference directly influences the resting potential and polarization of neurons, rendering it a pivotal factor affecting the electrical excitability of neurons [27]. Within 0–24 h, noncytotoxic concentrations of SNPs induced a sustained increase in CMP difference (Fig. 6), which indicated cell hyperpolarization [28], thereby contributing to reduced electrical excitability (Fig. 4). At 48 h, a significant decrease in CMP difference was observed compared to that at 24 h ($P < 0.05$). This might be due to the cytotoxicity of SNPs at 48 h, as cell death is usually accompanied by a decrease in CMP difference [29].

The intracellular Ca^{2+} contents in all SNPs-treated groups were higher than those in the control group (Fig. 7). These results are consistent with the finding of Elżbieta Ziemińska et al. that 75 μg/mL SNPs that were 5–35 nm in size could lead to elevated Ca^{2+} levels in cerebellar granule cells due to overactivation of Ca^{2+} channels [30]. Moreover, the intracellular Ca^{2+} content at 48 h was significantly lower ($P < 0.05$) than that at 24 h. This might be attributed to the very significant increase in intracellular Ca^{2+} content at 24 h, which initiated negative feedback regulation, followed by inactivation of Ca^{2+} channels [31], resulting in a decrease in intracellular Ca^{2+} content at 48 h. Overload of intracellular Ca^{2+} leads to mitochondrial and cytoskeletal damage and even apoptosis [32, 33]. Moreover, Ca^{2+} is an important intracellular signaling molecule that can control neurotransmitter release, regulate the expression of various proteins and influence the excitability of neurons [34]. In the current paper, 200 μM SNPs applied to PC12 cells for 48 h were found to simultaneously induce grade 1 cytotoxicity (Fig. 2), very significantly increase V_{Th} (Fig. 4) and very significantly increase intracellular Ca^{2+} content (Fig. 7).

The mitochondrion is an important organelle in the cell, as it is the site of energy production and one of the important targets of nanoparticles to induce toxicity [2]. The MMP difference is an important indicator of mitochondrial function. A decreased MMP difference implies mitochondrial damage and is one of the early signs of apoptosis [35]. Additionally, impaired mitochondria can lead to a decrease in ATP (an important cellular energy source) content, which subsequently can lead to cellular energy deficiency [36]. A previous study by our group found that the ATP content of human dermal fibroblasts decreased under the effect of SNPs [37]. Moreover, electrons escaping from a damaged mitochondrial electron transport chain might directly react with substances such as oxygen and generate ROS [38]. Damage to mitochondria therefore leads to increases in ROS content, and excessive ROS levels might contribute to further cellular damage (e.g., DNA, protein, and synaptic damage) [39]. Thus, ROS content is one of the most important indicators of cellular damage and the effect of nanoparticles on cells. The results displayed in Table 6 and Fig. 8 indicate that treatment with SNPs for 24 and 48 h caused mitochondrial damage which reduced the MMP difference, contributing to decreases in ATP content and increases in ROS content. Additionally, the MMP difference and ATP content of cells exposed to SNPs were very significantly higher ($P < 0.01$) than those of the control groups at 0.5 h of treatment, which could have been caused by the metabolic adaptation to the presence of SNPs. The metabolic adaptation might increase the MMP difference and enhance tricarboxylic acid cycle of mitochondria, resulting in increased ATP production [40].

The three indicators most highly correlated with cell viability in Table 7 were ATP content (r = 0.95), neurite length (r = 0.93), and ROS content (r=-0.90). SNPs have been found to simultaneously decrease ATP content and suppress neurite growth in human embryonic stem cell-derived neurons [41], and to decrease MMP difference, increase ROS content and decrease viability in A549 cells [42]. The current paper demonstrated that ATP content, neurite length and ROS content were important indicators of cellular damage caused by nanoparticles, and that the main cause of SNPs-induced cytotoxicity was the detrimental effects on cellular energy supply, cytoskeletal integrity and the ROS content.

Elevated intracellular Ca^{2+} content have been found to contribute to reduced ATP synthesis [32] and cellular energy deficiencies, which in turn open ATP-sensitive potassium (K_{ATP}) channels on the cell membrane, resulting in increases in CMP difference and hyperpolarization [28]. This paper showed that SNPs increased intracellular Ca^{2+} content (Fig. 7), decreased ATP content (Fig. 5), increased CMP difference (Fig. 6) and increased V_{Th} (Fig. 4) in PC12 cells. Furthermore, the three indicators most highly correlated with V_{Th} (displayed in Table 7) were intracellular Ca^{2+} content (r = 0.96), ATP content (r=-0.92) and CMP difference (r = 0.91). The above results suggest that the SNPs-induced decrease in electrical excitability may be explained by a decrease in ATP content due to an increase in intracellular Ca^{2+} content, which led to cellular energy deficiency that opened K_{ATP} channels on the cell membrane, resulting in an increase in CMP difference and hyperpolarization.

Additionally, ATP content was the only cytological indicator that correlated with both cell viability and V_{Th}, with correlation coefficients above 0.9. This result indicates that the ATP content was the main cytological indicator that affected both cytotoxicity and electrical excitability in the presence of SNPs, and illustrates the importance of energy supply for the maintenance of neuronal cell structure and function.

Possible mechanisms for the SNPs-induced changes in cytotoxicity and electrical excitability of PC12 cells are summarized in Fig. 9. SNPs decreased neurite length in PC12 cells, suggesting that SNPs caused cytoskeletal damage [25] and cytotoxicity. In addition, decreased neurite length might lead to a reduction in voltage-gated sodium channels and diminish the electrical excitability of PC12 quasi-neuronal networks [12]. The SNPs-induced decrease in MMP difference led to an increase in ROS content, which might damage biomolecules such as DNA and proteins, leading to cell death [39]. Moreover, increased ROS content might impair synaptic structures, which could affect intercellular signaling [43] and reduce the electrical excitability of PC12 quasi-neuronal networks. Both the decrease in MMP difference and the increase in intracellular Ca^{2+} content could lead to a decrease in ATP content. Decreased ATP content could lead to cellular energy deficiency, which both could activate apoptotic pathways [44], causing a decrease in cell viability, and could open K_{ATP} channels [28], causing an increase in CMP difference and hyperpolarization, eventually resulting in reduced electrical excitability.

Conclusion

In this paper, the effects of SNPs on the viability and electrical excitability of PC12 cells were investigated using the MTT method and VTMM. SNPs were found to alter the electrical excitability of PC12 quasi-neuronal networks at noncytotoxic concentrations. At the cytotoxic concentration, SNPs altered electrical excitability before they altered cell viability, suggesting that using only cell viability to evaluate nanoparticles-induced neurotoxicity is partial. Therefore, not only cell viability but also electrophysiological properties should be considered when evaluating nanoparticles-induced neurotoxicity. Further experiments revealed that the main reason for SNPs-induced cytotoxicity was the detrimental effects on cellular energy supply, cytoskeletal integrity and ROS content. The SNPs-induced decrease in electrical excitability could be explained by a decrease in ATP content caused by mitochondrial damage and caused by increased intracellular Ca^{2+} content. A decrease in ATP content could lead to cellular energy deficiency that opened K_{ATP} channels on the cell membrane, resulting in an increase in the CMP difference and hyperpolarization. ATP content was the main cytological indicator of both cytotoxicity and electrical excitability in the presence of SNPs.

Methods

Preparation and characterization of SNPs

SNPs were prepared by the sodium borohydride reduction of silver nitrate [20]. The morphology of SNPs was obtained using TEM (JEOL JEM-2100, Japan), and size analysis was performed using Image-Pro Plus software v 6.0 (Media Cybernetics, Inc., USA). The concentration of SNPs was measured using an inductive coupled plasma-optical emission spectrometer (Optima 5300DV, Perkin Elmer, USA).

Cell culture

Differentiated PC12 cells were purchased from Shanghai Cell Bank of Chinese Academy of Sciences. The cells were cultured in high-glucose DMEM (HyClone, United States) plus 10% fetal bovine serum (Biological Industries, Israel) and 1% (v/v) penicillin-streptomycin (Biological Industries, Israel), and were incubated in a 37°C, 5% CO_2 incubator with saturated humidity (Thermo Forma 3111, Thermo Fisher Scientific, United States). The experiments were performed with cells in logarithmic growth phase.

Evaluation of SNPs-induced cytotoxicity in PC12 cells

PC12 cells (100 μL/well) at a concentration of 6×10^4 cells/ml were added to a 96-well plate. After 24 h, the culture medium was aspirated, 5, 25, 50, 100 or 200 μM SNPs were added, and PC12 cells were then treated for another 0.5, 1, 12, 24 or 48 h. The cytotoxicity of SNPs was evaluated by the MTT method [45]. Cells cultured in medium without SNPs were used as the negative control, and cells cultured in medium containing 0.7% acrylamide were used as the positive control. Six parallel experiments were conducted for each concentration at each time point.

Preparation of PC12 quasi-neuronal networks on MEAs

At the beginning of each experiment, the MEA (60MEA100/10iR-Ti, Multi Channel Systems MCS GmbH, Germany) was immersed in 75% ethanol for 30 min, dried, and sterilized using ultraviolet light for 8 h. Next, the MEA chamber was filled with sufficient 0.1 mg/mL poly-L-lysine solution (Sigma-Aldrich, U.S.) to cover all the electrodes. Then, the MEA was placed in an incubator at 37°C with 5% CO_2 and saturated humidity for 24 h. Finally, the poly-L-lysine was removed, and the MEA was rinsed with sterilized ultra-pure water and dried in a laminar flow cabinet.

To build PC12 quasi-neuronal networks, 20 μL of differentiated PC12 cells with quasi-neuronal features were seeded onto the surface of the prepared MEA at a cell density of 1×10^6 cells/mL. Then, the MEA with PC12 cells was placed in an incubator and cultured with the culture medium for approximately 24 h at 37°C with 5% CO_2 and saturated humidity. The following experiments could be performed when the PC12 quasi-neuronal networks developed well and covered most of the electrode area on the MEA.

Measurement of standard V_{Th}

The experimental procedure and the selection of the voltage stimulation waveform for measuring the normal V_{Th} through VTMM are detailed in our previous paper [11, 12]. In brief, voltage stimulation from one selected stimulating electrode was generated by a voltage pulse generator (Agilent 33220A, USA), and used to trigger responses from the networks (Fig. 10A). The stimulation was an asymmetric charge-balanced biphasic pulse at 50 Hz with a positive phase of 2.00 ms and a negative phase of 0.20 ms (Fig. 10B). The amplitude of the negative pulse started at 0 mV and increased in steps of 1 mV. An oscilloscope (Agilent 2024A, USA) was used to supervise, recognize, and record the stimulation from the stimulating electrode and the responses from three selected detecting electrodes in real time (Fig. 10A). The minimum amplitude of the negative phase of the stimulation pulses that triggered responses from the networks in normal culture environment (with no exogenous factors) was defined as the standard V_{Th}. Each MEA was used only once. Four parallel experiments were conducted.

Measurement of V_{Th} of networks exposed to SNPs

The original culture medium in the MEA chamber was replaced with fresh test culture medium containing 5, 100 or 200 μM SNPs. After 0.5, 1, 12, 24 or 48 h of incubation, the V_{Th} of the networks was measured as described in Section 2.5. Four parallel experiments were conducted to measure the V_{Th} for each time point under each SNP concentration.

Measurement of neurite length of cells exposed to SNPs

PC12 cells (100 μL/well) at a concentration of 6×10^4 cells/ml were added to a 96-well plate. After 24 h, the culture medium was aspirated, and 200 μM SNPs were added. After PC12 cells were treated for another 0.5, 1, 12, 24 or 48 h, the culture medium was removed, and the cells were stained with TRITC-conjugated phalloidin and DAPI (Millipore, USA) [46]. The average neurite length was analysed with a HCA system (Array XTI, Thermo Fisher, USA). Cells cultured in medium without SNPs were used as the negative control. Six parallel experiments were conducted for each time point.

Measurement of CMP difference of cells exposed to SNPs

The CMP difference was monitored by bis-(1,3-dibutylbarbituric acid) trimethine oxonol ($DiBAC_4(3)$) (B438, Molecular Probes, United States). $DiBAC_4(3)$ stock solution (20 mM, dissolved in dimethylsulfoxide) was diluted in Hank's balanced salt solution (C0218, Beyotime, China) to working solution (40 μM). PC12 cells were stained with $DiBAC_4(3)$ working solution in 96-well plates (100 μL/well, 1 h) after 0.5, 1, 12, 24 or 48 h treatment with 200 μM SNPs [47]. The average fluorescence intensity of $DiBAC_4(3)$ was measured with the HCA system. Cells cultured in medium without SNPs were used as the negative control. Six parallel experiments were conducted for each time point.

Measurement of intracellular Ca^{2+} content of cells exposed to SNPs

PC12 cells were stained using Fluo-3 AM (S1056, Beyotime, China) in 96-well plates after treatment with 200 μM SNPs for 0.5, 1, 12, 24 or 48 h [48]. The average fluorescence intensity of the probes was measured with the HCA system. Cells cultured in medium without SNPs were used as the negative control. Six parallel experiments were conducted for each time point.

Measurement of MMP difference, ATP content, and ROS content of cells exposed to SNPs

JC-1 (C2006, Beyotime, China) was used to stain PC12 cells after treatment with 200 μM SNPs for 0.5, 1, 12, 24 or 48 h [49]. The average fluorescence intensity of JC-1 aggregates (which produce red fluorescence) and monomers (which produce green fluorescence) was measured with the HCA system. Cells cultured in medium without SNPs were used as the negative control. Six parallel experiments were conducted for each time point.

The ATP content was measured using an ATP assay kit (S0026, Beyotime, China). PC12 cells (1 ml/well) at a concentration of 6×10^4/ml were cultured in a 12-well plate. After 24 h, the culture solution was aspirated, and 1 ml of 200 μM SNPs was added. After 0.5, 1, 12, 24 or 48 h of treatment, the cells were lysed, and the supernatants were collected. The ATP concentrations (C_{ATP}) and protein concentrations ($C_{Protein}$) were then detected, and the ATP content was determined as $C_{ATP}/C_{Protein}$ and expressed in nmol/mg [50]. Cells cultured in medium without SNPs were used as the negative control. Six parallel experiments were conducted for each time point.

An ROS Assay Kit (S0033S, Beyotime, China) was used to stain PC12 cells in 96-well plates after treatment with 200 μM SNPs for 0.5, 1, 12, 24 or 48 h [50]. The average fluorescence intensity of dichlorofluorescein generated by the oxidation of ROS was measured with the HCA system. Cells cultured in medium without SNPs were used as the negative control. Six parallel experiments were conducted for each time point.

Data processing and analysis

The Shapiro-Wilk test was employed to test the distribution of the results from parallel groups for normality via SPSS 20.0 software (IBM, Armonk, NY, USA). All experimental data are expressed as the mean ± SD. Student's t test was performed unless otherwise noted. $P < 0.05$ was considered to indicate a significant difference, and $P < 0.01$ was considered to indicate a very significant difference. All experiments were repeated at least three times. Pearson correlation analysis was used for correlation analysis of datasets. The correlation coefficient is abbreviated as "r"; $|r| = 0.8$ to 1.0 indicates high correlations, $|r| = 0.5$ to 0.8 indicates moderate correlations, $|r| = 0.3$ to 0.5 indicates low correlations and $|r| = 0$ to 0.3 indicates very weak or no correlations [51].

Abbreviations

SNPs
Silver nanoparticles
MEA
Microelectrode array
VTMM
Voltage threshold measurement method
V_{Th}
Voltage threshold
PC12 cells
Rat adrenal pheochromocytoma cells
CMP
Cell membrane potential
MMP
Mitochondrial membrane potential
ATP
Adenosine triphosphate
ROS
Reactive oxygen species
HCA
High content analysis
TEM
Transmission electron microscopy
SD
Standard deviation
K_{ATP} channels
ATP-sensitive potassium channels
DiBAC4(3)
Bis-(1,3-dibutylbarbituric acid) trimethine oxonol
C_{ATP}

ATP concentrations

$C_{Protein}$

Protein concentrations.

Declarations

Ethics approval and consent to participate

Not applicable.

Consent for publication

Not applicable.

Availability of data and materials

The datasets supporting the conclusions of this article are included within the article and its additional files.

Competing interests

The authors declare that they have no known competing financial interests or personal relationships that could have appeared to influence the work reported in this paper.

Funding

This study was supported by the National Natural Sciences Foundation of China (grant no. 61874024, 61534003, 61076118).

Authors' contributions

Ze-Qun Zhang: Formal analysis, Data curation, Validation, Investigation, Visualization, Writing – original draft and Writing – review & editing.

Chen Meng: Investigation and Validation.

Kun Hou: Investigation and Validation.

Zhi-Gong Wang: Supervision, Conceptualization, Methodology, Project administration and Funding acquisition.

Yan Huang: Supervision, Methodology, Validation and Writing – review & editing.

Xiao-Ying Lü: Supervision, Conceptualization, Methodology, Validation, Project administration, Funding acquisition and Writing – review & editing.

Zhi-Gong Wang, Yan Huang and Xiao-Ying Lü are Corresponding authors.

All authors read and approved the final manuscript.

References

1. Ge LP, Li QT, Wang M, Ouyang J, Li XJ, Xing MMQ. Nanosilver particles in medical applications: synthesis, performance, and toxicity. Int J Nanomed. 2014;9:2399–407. doi: 10.2147/ijn.S55015.
2. Ahari H, Lahijani LK. Migration of Silver and Copper Nanoparticles from Food Coating. Coatings. 2021;11(4):380. doi: 10.3390/coatings11040380.
3. Jennifer M, Maciej W. Nanoparticle Technology as a Double-Edged Sword: Cytotoxic, Genotoxic and Epigenetic Effects on Living Cells. Journal of Biomaterials and Nanobiotechnology. 2013;Vol.04No.01:11. doi: 10.4236/jbnb.2013.41008.
4. Struzynska L, Skalska J. Mechanisms Underlying Neurotoxicity of Silver Nanoparticles. Adv Exp Med Biol. 2018;1048:227–50. doi: 10.1007/978-3-319-72041-8_14.
5. Berti L, Bonfioli E, Chioffi L, Morgante S, Mazzi MA, Burti L. Lifestyles of Patients with Functional Psychosis Compared to Those of a Sample of the Regional General Population: Findings from a Study in a Community Mental Health Service of the Veneto Region, Italy. Community Mental Health Journal. 2018;54(7):1050–6. doi: 10.1007/s10597-017-0223-7.
6. Pavicic I, Milic M, Pongrac IM, Ahmed LB, Glavan TM, Ilic K, et al. Neurotoxicity of silver nanoparticles stabilized with different coating agents: In vitro response of neuronal precursor cells. Food Chem Toxicol. 2020;136:110935. doi: 10.1016/j.fct.2019.110935.
7. Strickland JD, LeFew WR, Crooks J, Hall D, Ortenzio JNR, Dreher K, et al. In vitro screening of silver nanoparticles and ionic silver using neural networks yields differential effects on spontaneous activity and pharmacological responses. Toxicology. 2016;355:1–8. doi: 10.1016/j.tox.2016.05.009.
8. Thomas CA, Jr., Springer PA, Loeb GE, Berwald-Netter Y, Okun LM. A miniature microelectrode array to monitor the bioelectric activity of cultured cells. Exp Cell Res. 1972;74(1):61–6. doi: 10.1016/0014-4827(72)90481-8.
9. Johnstone AFM, Gross GW, Weiss DG, Schroeder OHU, Gramowski A, Shafer TJ. Microelectrode arrays: A physiologically based neurotoxicity testing platform for the 21st century. Neurotoxicology. 2010;31(4):331–50. doi: 10.1016/j.neuro.2010.04.001.
10. Kay GN, Shepard RB. Chapter 1 - Cardiac Electrical Stimulation. In: Ellenbogen KA, Kay GN, Lau C-P, Wilkoff BL, editors. Clinical Cardiac Pacing, Defibrillation, and Resynchronization Therapy (Third Edition). Philadelphia: W.B. Saunders; 2007. p. 3–58.
11. An S, Zhao YF, Lu XY, Wang ZG. Quantitative evaluation of extrinsic factors influencing electrical excitability in neuronal networks: Voltage Threshold Measurement Method (VTMM). Neural Regen Res. 2018;13(6):1026–35. doi: 10.4103/1673-5374.233446.
12. Lü X-Y, Hou K, Zhao Y-F, An S, Wang Z-G. Conjoint analysis of influence of LC-HCL and Mor-HCL on Vth and neurite length in hippocampal neuronal network. Neuroscience Letters. 2021;751:135801.

doi: 10.1016/j.neulet.2021.135801.

13. Greene LA, Tischler AS. Establishment of a noradrenergic clonal line of rat adrenal pheochromocytoma cells which respond to nerve growth factor. Proc Natl Acad Sci U S A. 1976;73(7):2424–8. doi: 10.1073/pnas.73.7.2424.
14. Zhao W, Cui W, Xu S, Cheong L-Z, Wang D, Shen C. Direct study of the electrical properties of PC12 cells and hippocampal neurons by EFM and KPFM. Nanoscale Advances. 2019;1(2):537–45. doi: 10.1039/c8na00202a.
15. Westerink RHS, Ewing AG. The PC12 cell as model for neurosecretion. Acta Physiologica. 2008;192(2):273–85. doi: 10.1111/j.1748-1716.2007.01805.x.
16. Liu Y, Li J, Xu K, Gu J, Huang L, Zhang L, et al. Characterization of superparamagnetic iron oxide nanoparticle-induced apoptosis in PC12 cells and mouse hippocampus and striatum. Toxicol Lett. 2018;292:151–61. doi: 10.1016/j.toxlet.2018.04.033.
17. Gu C, Ewing AG. Simultaneous detection of vesicular content and exocytotic release with two electrodes in and at a single cell. Chemical Science. 2021;12(21):7393–400. doi: 10.1039/d1sc01190a.
18. Cui MR, Zhao W, Li XL, Xu CH, Xu JJ, Chen HY. Simultaneous monitoring of action potentials and neurotransmitter release from neuron-like PC12 cells. Analytica Chimica Acta. 2020;1105:74–81. doi: 10.1016/j.aca.2019.11.074.
19. Xiaoying Lü, Chen Meng, Shuai An, Yong-Fang Zhao, Wang Z-G. Study on influence of external factors on the electrical excitability of PC12 quasi-neuronal networks through Voltage Threshold Measurement Method. PloS one. 2022;17(3):e0265078. doi: 10.1371/journal.pone.0265078.
20. Ma JW, Lu XY, Huang Y. Genomic Analysis of Cytotoxicity Response to Nanosilver in Human Dermal Fibroblasts. Journal of Biomedical Nanotechnology. 2011;7(2):263–75. doi: 10.1166/jbn.2011.1286.
21. Liu F, Mahmood M, Xu Y, Watanabe F, Biris AS, Hansen DK, et al. Effects of silver nanoparticles on human and rat embryonic neural stem cells. Frontiers in Neuroscience. 2015;9:115. doi: 10.3389/fnins.2015.00115.
22. Zhang B, Liu N, Liu QS, Zhang J, Zhou Q, Jiang G. Silver nanoparticles induce size-dependent and particle-specific neurotoxicity to primary cultures of rat cerebral cortical neurons. Ecotox Environ Safe. 2020;198:110674. doi: 10.1016/j.ecoenv.2020.110674.
23. Kun Hou CM, Yan Huang, Xiao-Ying Lü, Zhi-Gong Wang. Study of effect of silver nanoparticles on the electrical excitability of hippocampal neuronal network based on “Voltage Threshold Measurement Method”. 2021 IEEE International Biomedical Instrumentation and Technology Conference (IBITeC). Virtually2021. p. 1–5.
24. Kole MHP, Ilschner SU, Kampa BM, Williams SR, Ruben PC, Stuart GJ. Action potential generation requires a high sodium channel density in the axon initial segment. Nature Neuroscience. 2008;11(2):178–86. doi: 10.1038/nn2040.
25. Cooper RJ, Menking-Colby MN, Humphrey KA, Victory JH, Kipps DW, Spitzer N. Involvement of beta-catenin in cytoskeleton disruption following adult neural stem cell exposure to low-level silver

nanoparticles. Neurotoxicology. 2019;71:102–12. doi: 10.1016/j.neuro.2018.12.010.

26. Rafieepour A, Azari MR, Peirovi H, Khodagholi F, Jaktaji JP, Mehrabi Y, et al. Investigation of the effect of magnetite iron oxide particles size on cytotoxicity in A(549) cell line. Toxicology and Industrial Health. 2019;35(11–12):703–13. doi: 10.1177/0748233719888077.
27. Kadir LA, Stacey M, Barrett-Jolley R. Emerging Roles of the Membrane Potential: Action Beyond the Action Potential. Frontiers in Physiology. 2018;9:1661. doi: 10.3389/fphys.2018.01661.
28. Sun H-s, Feng Z-p. Neuroprotective role of ATP-sensitive potassium channels in cerebral ischemia. Acta Pharmacologica Sinica. 2013;34(1):24–32. doi: 10.1038/aps.2012.138.
29. Adebodun F, Post JFM. F-19 NMR-STUDIES OF CHANGES IN MEMBRANE-POTENTIAL AND INTRACELLULAR VOLUME DURING DEXAMETHASONE-INDUCED APOPTOSIS IN HUMAN LEUKEMIC-CELL LINES. Journal of Cellular Physiology. 1993;154(1):199–206. doi: 10.1002/jcp.1041540123.
30. Zieminska E, Stafiej A, Struzynska L. The role of the glutamatergic NMDA receptor in nanosilver-evoked neurotoxicity in primary cultures of cerebellar granule cells. Toxicology. 2014;315:38–48. doi: 10.1016/j.tox.2013.11.008.
31. Ehlers MD, Zhang S, Bernhardt JP, Huganir RL. Inactivation of NMDA receptors by direct interaction of calmodulin with the NR1 subunit. Cell. 1996;84(5):745–55. doi: 10.1016/s0092-8674(00)81052-1.
32. Brookes PS, Yoon YS, Robotham JL, Anders MW, Sheu SS. Calcium, ATP, and ROS: a mitochondrial love-hate triangle. American Journal of Physiology-Cell Physiology. 2004;287(4):C817-C33. doi: 10.1152/ajpcell.00139.2004.
33. Genchi G, Sinicropi MS, Lauria G, Carocci A, Catalano A. The Effects of Cadmium Toxicity. International Journal of Environmental Research and Public Health. 2020;17(11):3782. doi: 10.3390/ijerph17113782.
34. Bornschein G, Schmidt H. Synaptotagmin Ca2 + Sensors and Their Spatial Coupling to Presynaptic Ca-v Channels in Central Cortical Synapses. Frontiers in Molecular Neuroscience. 2019;11:494. doi: 10.3389/fnmol.2018.00494.
35. Zamzami N, Marchetti P, Castedo M, Zanin C, Vayssiere JL, Petit PX, et al. REDUCTION IN MITOCHONDRIAL POTENTIAL CONSTITUTES AN EARLY IRREVERSIBLE STEP OF PROGRAMMED LYMPHOCYTE DEATH IN-VIVO. Journal of Experimental Medicine. 1995;181(5):1661–72. doi: 10.1084/jem.181.5.1661.
36. Rolfe DFS, Brown GC. Cellular energy utilization and molecular origin of standard metabolic rate in mammals. Physiological Reviews. 1997;77(3):731–58.
37. Huang Y, Lu XY, Lu XQ. Cytotoxic Mechanism for Silver Nanoparticles Based High-Content Cellomics and Transcriptome Sequencing. Journal of Biomedical Nanotechnology. 2019;15(7):1401–14. doi: 10.1166/jbn.2019.2785.
38. Murphy MP. How mitochondria produce reactive oxygen species. Biochemical Journal. 2009;417:1–13. doi: 10.1042/bj20081386.
39. Valko M, Leibfritz D, Moncol J, Cronin MTD, Mazur M, Telser J. Free radicals and antioxidants in normal physiological functions and human disease. International Journal of Biochemistry & Cell

Biology. 2007;39(1):44–84. doi: 10.1016/j.biocel.2006.07.001.

40. Jarak I, Carrola J, Barros AS, Gil AM, Pereira MD, Corvo ML, et al. From the Cover: Metabolism Modulation in Different Organs by Silver Nanoparticles: An NMR Metabolomics Study of a Mouse Model. Toxicological Sciences. 2017;159(2):422–35. doi: 10.1093/toxsci/kfx142.
41. Repar N, Li H, Aguilar JS, Li QQ, Drobne D, Hong Y. Silver nanoparticles induce neurotoxicity in a human embryonic stem cell-derived neuron and astrocyte network. Nanotoxicology. 2018;12(2):104–16. doi: 10.1080/17435390.2018.1425497.
42. Han JW, Gurunathan S, Jeong JK, Choi YJ, Kwon DN, Park JK, et al. Oxidative stress mediated cytotoxicity of biologically synthesized silver nanoparticles in human lung epithelial adenocarcinoma cell line. Nanoscale Research Letters. 2014;9:459. doi: 10.1186/1556-276x-9-459.
43. Massaad CA, Klann E. Reactive Oxygen Species in the Regulation of Synaptic Plasticity and Memory. Antioxidants & Redox Signaling. 2011;14(10):2013–54. doi: 10.1089/ars.2010.3208.
44. Nicotera P, Leist M, Ferrando-May E. Intracellular ATP, a switch in the decision between apoptosis and necrosis. Toxicol Lett. 1998;103:139–42.
45. Lu XY, Bao X, Huang Y, Qu YH, Lu HQ, Lu ZH. Mechanisms of cytotoxicity of nickel ions based on gene expression profiles. Biomaterials. 2009;30(2):141–8. doi: 10.1016/j.biomaterials.2008.09.011.
46. Ghezzi B, Lagonegro P, Fukata N, Parisi L, Calestani D, Galli C, et al. Sub-Micropillar Spacing Modulates the Spatial Arrangement of Mouse MC3T3-E1 Osteoblastic Cells. Nanomaterials. 2019;9(12):1701. doi: 10.3390/nano9121701.
47. Pai VHP, Cervera J, Mafe S, Willocq V, Lederer EK, Levin M. HCN2 Channel-Induced Rescue of Brain Teratogenesis via Local and Long-Range Bioelectric Repair. Frontiers in Cellular Neuroscience. 2020;14:136. doi: 10.3389/fncel.2020.00136.
48. Liu Y, Li J, Chen H, Cai Y, Sheng T, Wang P, et al. Magnet-activatable nanoliposomes as intracellular bubble microreactors to enhance drug delivery efficacy and burst cancer cells. Nanoscale. 2019;11(40):18854–65. doi: 10.1039/c9nr07021d.
49. Dang J, Ye H, Li Y, Liang Q, Li X, Yin L. Multivalency-assisted membrane-penetrating siRNA delivery sensitizes photothermal ablation via inhibition of tumor glycolysis metabolism. Biomaterials. 2019;223:119463. doi: 10.1016/j.biomaterials.2019.119463.
50. Huang Y, Lu XY, Chen R, Chen Y. Comparative study of the effects of gold and silver nanoparticles on the metabolism of human dermal fibroblasts. Regenerative Biomaterials. 2020;7(2):221–32. doi: 10.1093/rb/rbz051.
51. Overholser BR, Sowinski KM. Biostatistics primer: Part 2. Nutrition in Clinical Practice. 2008;23(1):76–84. doi: 10.1177/011542650802300176.

Figures

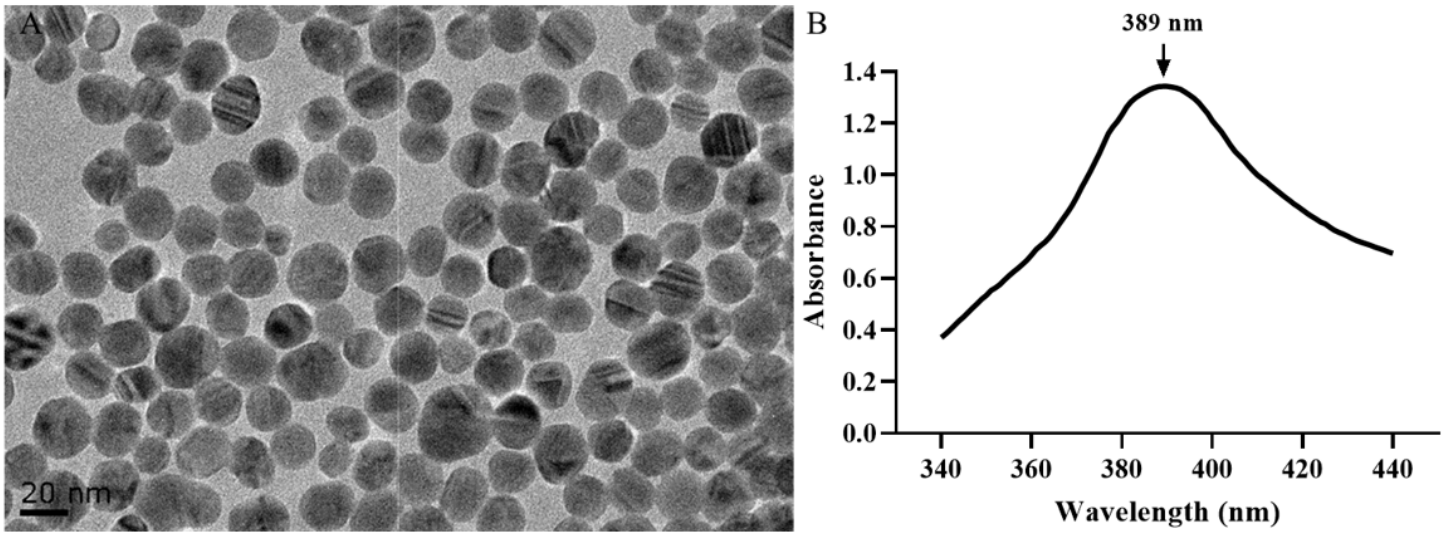

Figure 1

Characterization of SNPs. **A** TEM image of SNPs. **B** Absorption spectra of SNPs.

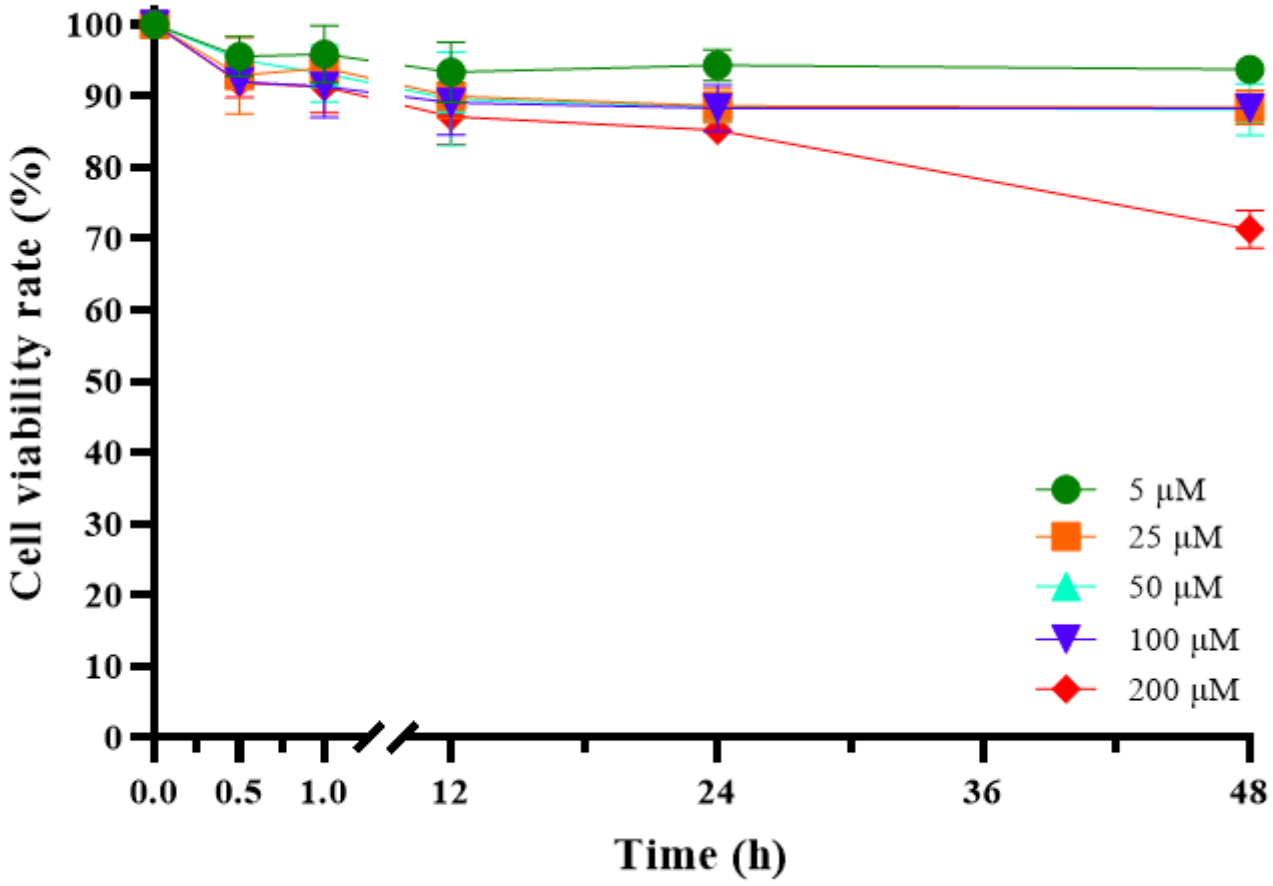

Figure 2

Cell viability rates of PC12 cells. The cell viability rates of PC12 cells treated with 20 nm SNPs at concentrations of 5, 25, 50, 100 and 200 μM for 0.5, 1, 12, 24 and 48 h. The results are presented as the mean ± SD (n= 6). Viability rate

[81%, 100%] indicates grade 0 cytotoxicity, viability rate

[61%, 80%] indicates grade 1 cytotoxicity, viability rate

[41%, 60%] indicates grade 2 cytotoxicity, viability rate

[21%, 40%] indicates grade 3 cytotoxicity, and viability rate

[0, 20%] indicates grade 4 cytotoxicity.

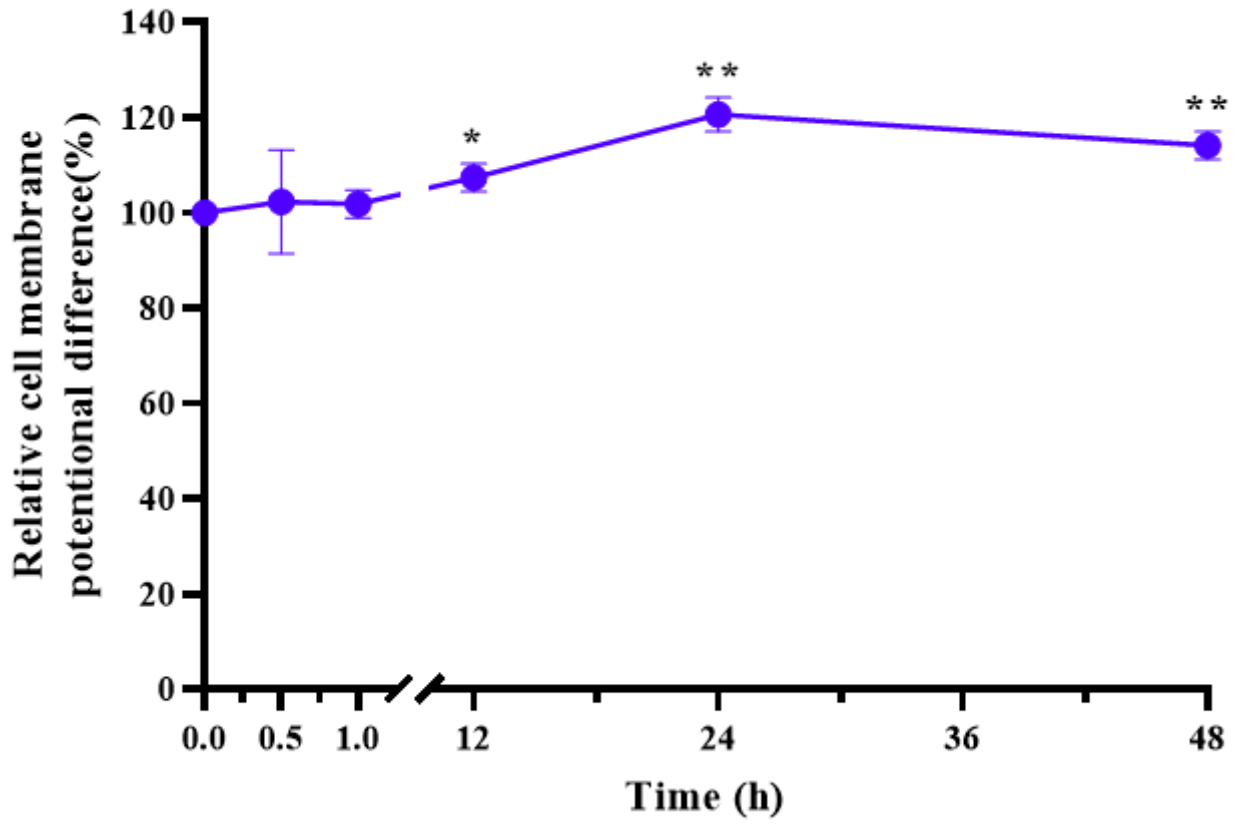

Figure 3

Image of PC12 quasi-neuronal networks on MEA and waveform shown by oscilloscope. **A** Image of PC12 quasi-neuronal networks on MEA, with stimulating electrode in the red box and detecting electrodes in the blue box. The locations of stimulating and detecting electrodes were not fixed in different MEA. Instead, according to the conditions of networks, the electrodes well covered by cells were randomly selected as the stimulating and detecting electrodes, respectively. **B** Waveform of the stimulation signal (yellow) and

response signals (green, blue and red) shown by oscilloscope in a normally cultured PC12 quasi-neuronal network (The dataset is shown in Additional file 2).

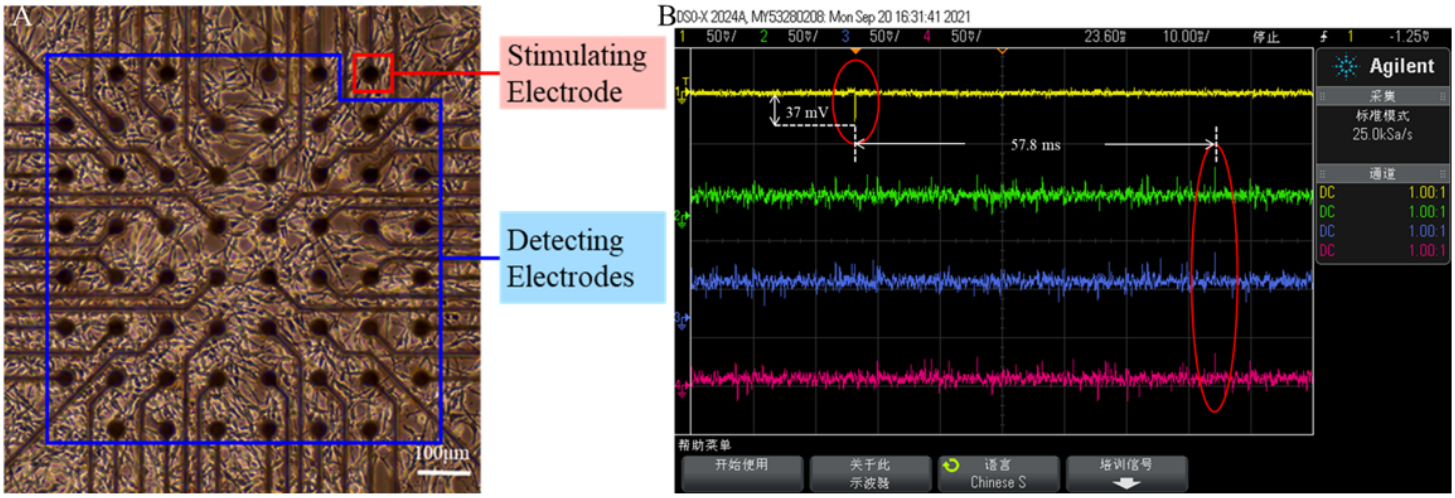

Figure 4

V_{Th} of PC12 quasi-neuronal networks. The V_{Th} of PC12 quasi-neuronal networks treated with 20 nm SNPs at concentrations of 5, 100 and 200 μM for 0.5, 1, 12, 24 and 48 h. * P< 0.05,** P< 0.01. The results are presented as the mean ± SD (n= 4).

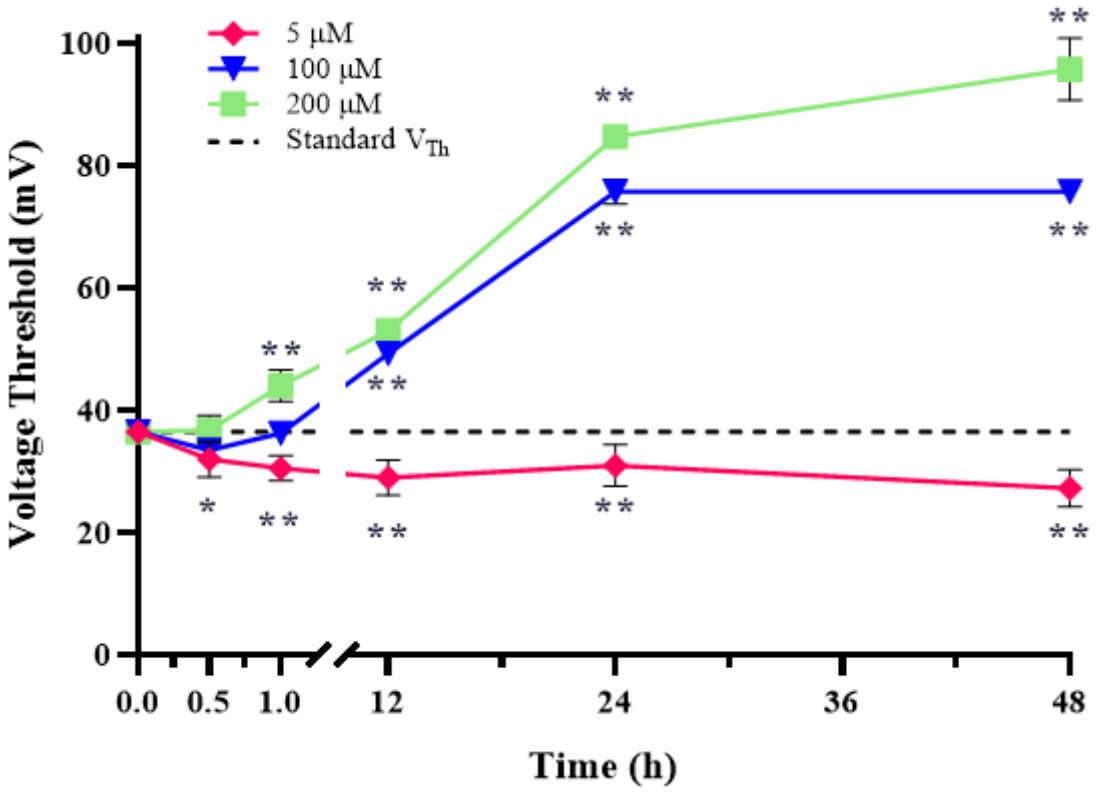

Figure 5

Neurite length of PC12 cells. The neurite length of PC12 cells treated with 20 nm 200 μM SNPs for 0.5, 1, 12, 24 and 48 h. * P< 0.05, ** P< 0.01. The results are presented as the mean ± SD (n= 6).

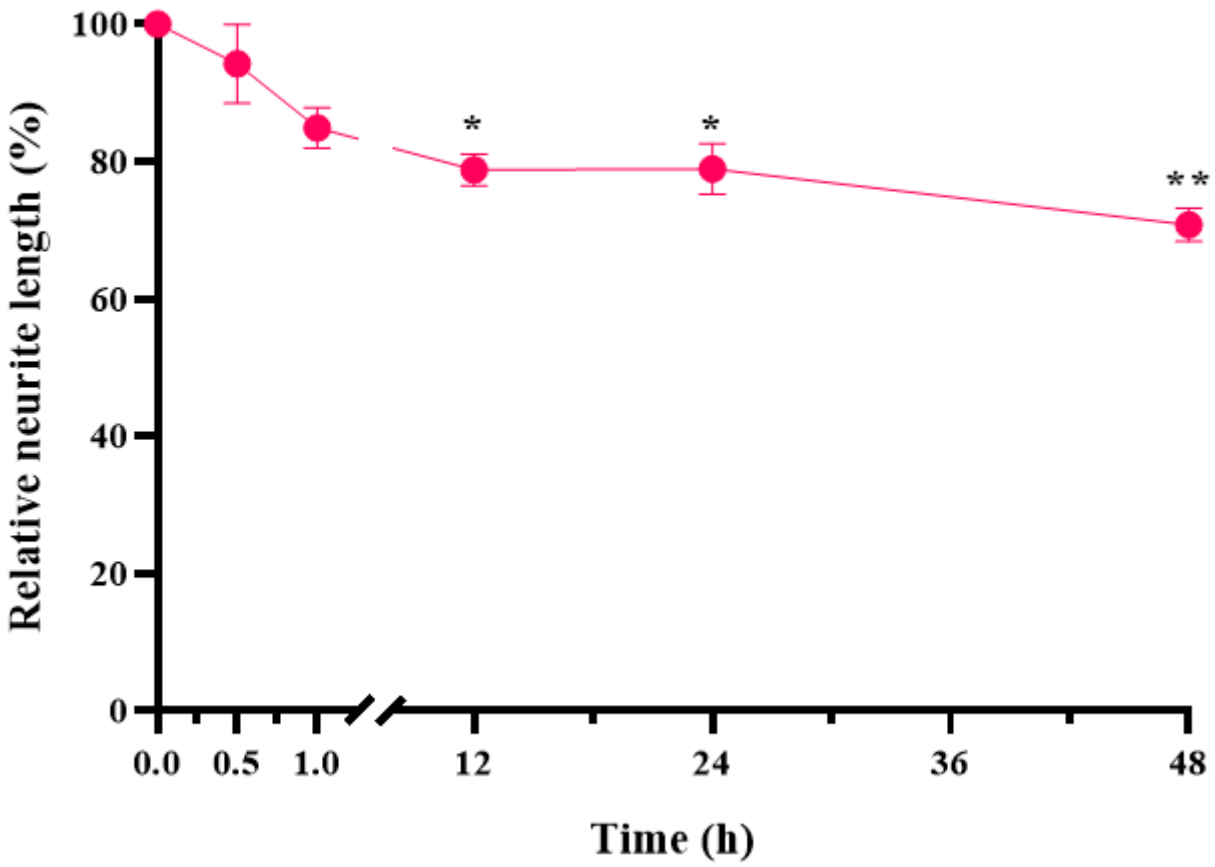

Figure 6

CMP difference of PC12 cells. The CMP difference of PC12 cells treated with 20 nm 200 μM SNPs for 0.5, 1, 12, 24 and 48 h. *P< 0.05,**P< 0.01. The results are presented as the mean ± SD (n= 6).

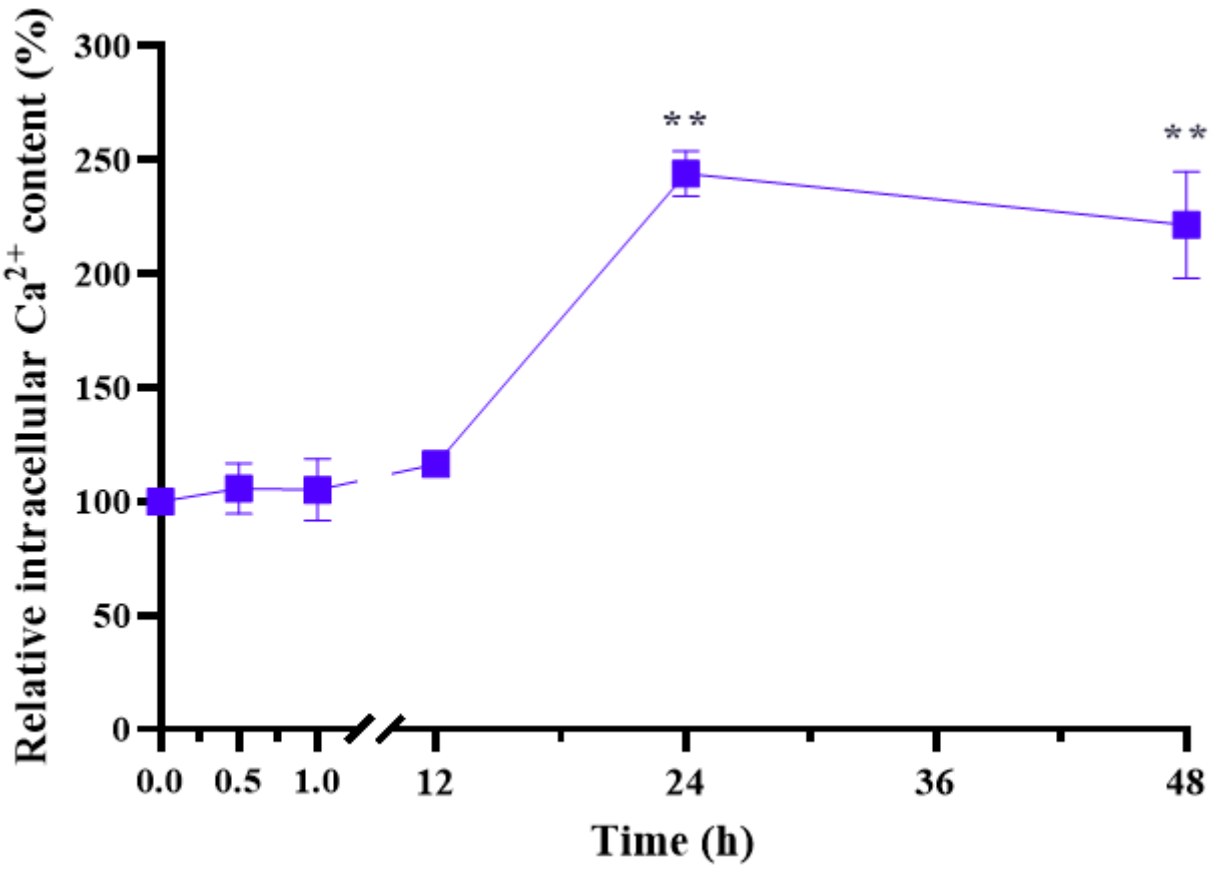

Figure 7

Intracellular Ca^{2+} content of PC12 cells. The intracellular Ca^{2+} content of PC12 cells treated with 20 nm 200 μM SNPs for 0.5, 1, 12, 24 and 48 h. ** P< 0.01. The results are presented as the mean ± SD (n= 6).

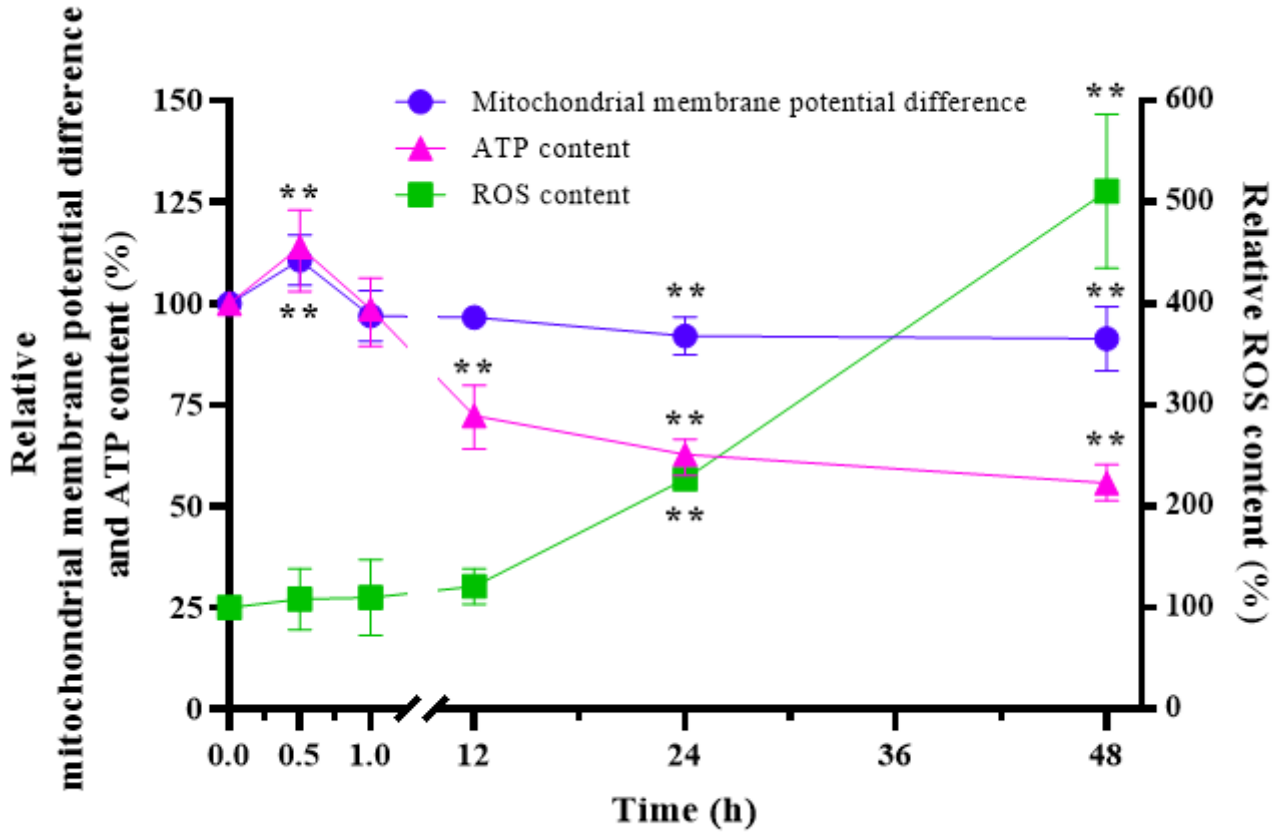

Figure 8

MMP difference, ATP content and ROS content of PC12 cells. MMP difference, ATP content and ROS content of PC12 cells treated with 20 nm 200 μM SNPs for 0.5, 1, 12, 24 and 48 h. *P< 0.05,**P< 0.01. The results are presented as the mean ± SD (n= 6).

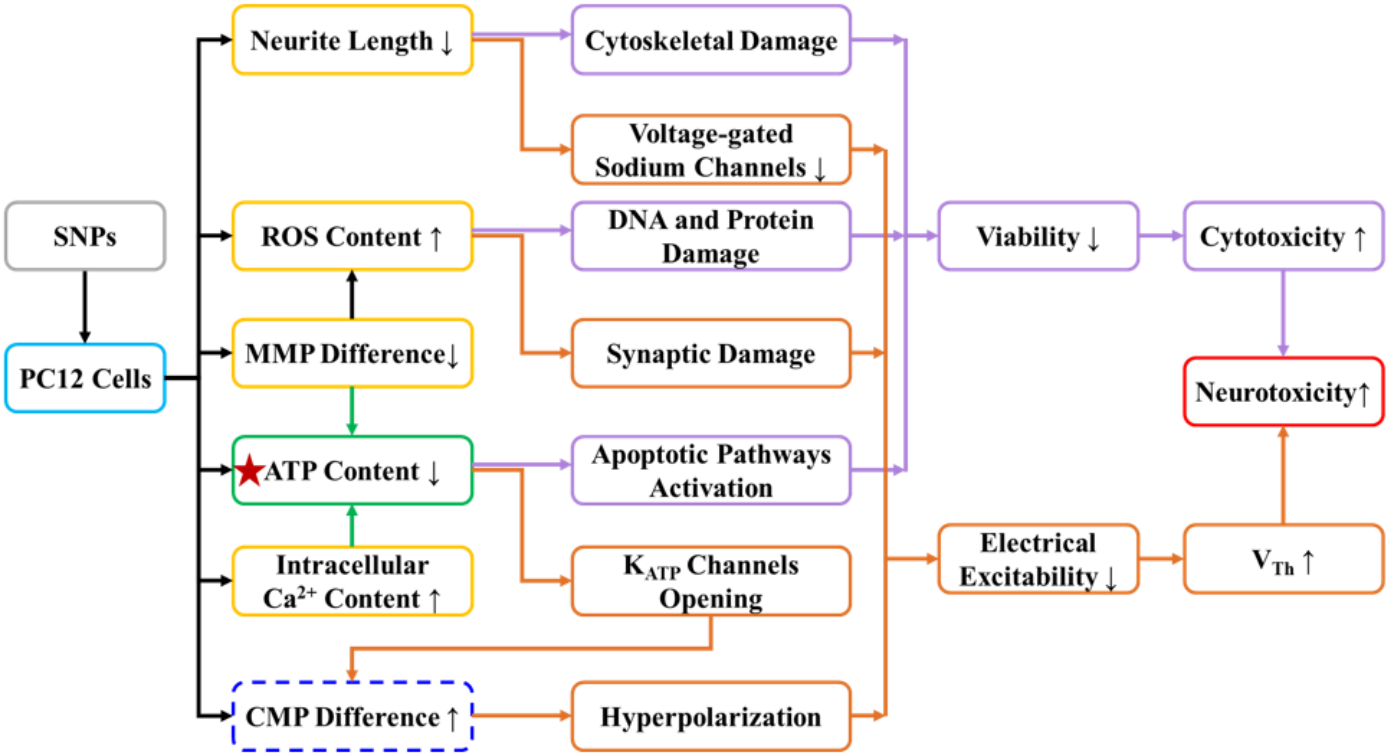

Figure 9

Diagram of possible mechanisms for the changes in cytotoxicity and electrical excitability of PC12 cells caused by SNPs.

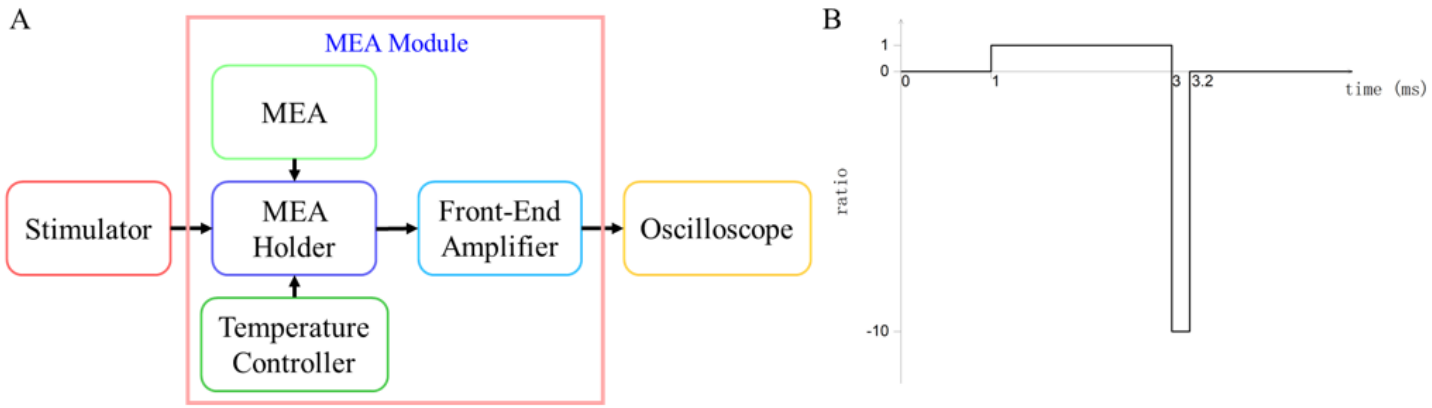

Figure 10

Block diagram showing VTMM system and the waveform of voltage stimulation. **A** Block diagram showing VTMM system. **B** The waveform of voltage stimulation. The stimulation was an asymmetric charge-balanced biphasic pulse at 50 Hz with a positive phase of 2.00 ms and a negative phase of 0.20 ms.

Supplementary Files

This is a list of supplementary files associated with this preprint. Click to download.

- Additionalfile1.xlsx
- Additionalfile2.csv
- Additionalfile2.docx
- Additionalfile3.csv